NAVAL POSTGRADUATE SCHOOL

MONTEREY, CALIFORNIA

THESIS

DYNAMIC DESIGN ANALYSIS METHOD AS A PREDICTION OF SYSTEM FAILURES

by

Brian F. Gottfried

December 2018

Thesis Advisor: Young W. Kwon
Co-Advisor: Jarema M. Didoszak

THIS PAGE INTENTIONALLY LEFT BLANK

REPORT DOCUMENTATION PAGE			*Form Approved OMB No. 0704-0188*
Public reporting burden for this collection of information is estimated to average 1 hour per response, including the time for reviewing instruction, searching existing data sources, gathering and maintaining the data needed, and completing and reviewing the collection of information. Send comments regarding this burden estimate or any other aspect of this collection of information, including suggestions for reducing this burden, to Washington headquarters Services, Directorate for Information Operations and Reports, 1215 Jefferson Davis Highway, Suite 1204, Arlington, VA 22202-4302, and to the Office of Management and Budget, Paperwork Reduction Project (0704-0188) Washington, DC 20503.			
1. AGENCY USE ONLY ***(Leave blank)***	**2. REPORT DATE** December 2018	**3. REPORT TYPE AND DATES COVERED** Master's thesis	
4. TITLE AND SUBTITLE DYNAMIC DESIGN ANALYSIS METHOD AS A PREDICTION OF SYSTEM FAILURES			**5. FUNDING NUMBERS**
6. AUTHOR(S) Brian F. Gottfried			
7. PERFORMING ORGANIZATION NAME(S) AND ADDRESS(ES) Naval Postgraduate School Monterey, CA 93943-5000			**8. PERFORMING ORGANIZATION REPORT NUMBER**
9. SPONSORING / MONITORING AGENCY NAME(S) AND ADDRESS(ES) N/A			**10. SPONSORING / MONITORING AGENCY REPORT NUMBER**
11. SUPPLEMENTARY NOTES The views expressed in this thesis are those of the author and do not reflect the official policy or position of the Department of Defense or the U.S. Government.			
12a. DISTRIBUTION / AVAILABILITY STATEMENT Approved for public release. Distribution is unlimited.			**12b. DISTRIBUTION CODE** A

13. ABSTRACT (maximum 200 words)

The ANSYS Mechanical program was used to model a simple structure representing shipboard equipment. A modal analysis and DDAM application were performed to determine the resulting displacements in the different modes of the systems. These displacements were then applied to the system in order to determine whether the combined modal displacements caused the critical component, represented by two thin beams, to make contact. If so, the system will have a predicted failure. The results were then compared to a NASTRAN time-dependent model for a solution comparison.

14. SUBJECT TERMS DDAM, LFT&E, modal analysis, shock trials, shock trial qualification, shock design, Dynamic Design Analysis Method			**15. NUMBER OF PAGES** 67
			16. PRICE CODE
17. SECURITY CLASSIFICATION OF REPORT Unclassified	**18. SECURITY CLASSIFICATION OF THIS PAGE** Unclassified	**19. SECURITY CLASSIFICATION OF ABSTRACT** Unclassified	**20. LIMITATION OF ABSTRACT** UU

NSN 7540-01-280-5500

Standard Form 298 (Rev. 2-89)
Prescribed by ANSI Std. 239-18

THIS PAGE INTENTIONALLY LEFT BLANK

Approved for public release. Distribution is unlimited.

DYNAMIC DESIGN ANALYSIS METHOD AS A PREDICTION OF SYSTEM FAILURES

Brian F. Gottfried
Lieutenant, United States Navy
BSE, University of South Carolina, 2011

Submitted in partial fulfillment of the
requirements for the degree of

MASTER OF SCIENCE IN MECHANICAL ENGINEERING

from the

NAVAL POSTGRADUATE SCHOOL
December 2018

Approved by: Young W. Kwon
Advisor

Jarema M. Didoszak
Co-Advisor

Garth V. Hobson
Chair, Department of Mechanical and Aerospace Engineering

THIS PAGE INTENTIONALLY LEFT BLANK

ABSTRACT

The ANSYS Mechanical program was used to model a simple structure representing shipboard equipment. A modal analysis and DDAM application were performed to determine the resulting displacements in the different modes of the systems. These displacements were then applied to the system in order to determine whether the combined modal displacements caused the critical component, represented by two thin beams, to make contact. If so, the system will have a predicted failure. The results were then compared to a NASTRAN time-dependent model for a solution comparison.

THIS PAGE INTENTIONALLY LEFT BLANK

TABLE OF CONTENTS

THIS PAGE INTENTIONALLY LEFT BLANK

LIST OF FIGURES

LIST OF TABLES

THIS PAGE INTENTIONALLY LEFT BLANK

LIST OF ACRONYMS AND ABBREVIATIONS

APDL	advanced programming design language
DDAM	Dynamic Design Analysis Method
DOF	degree of freedom
DSF	Deck Simulating Fixture
DSSM	Deck Simulating Shock Machine
FSP	Floating Shock Platform
FSST	Full Ship Shock Trial
LFT&E	Live Fire Test & Evaluation
LWSM	Lightweight Shock Machine
MHC	Mine Hunter Class
MWSM	Mediumweight Shock Machine
NRL	Naval Reactors Laboratories
RMS	root mean square
UNDEX	underwater non-contact explosion

THIS PAGE INTENTIONALLY LEFT BLANK

ACKNOWLEDGMENTS

I would like to extend my heartfelt appreciation to my loving and caring wife, Stephanie, whose constant encouragement and support was vital to my success and will undoubtedly continue to help me in my military career.

I'd also like to thank Professor Young Kwon, whose expertise in mechanical engineering as well as finite element modeling proved invaluable in generating the geometries, matrixes, and MATLAB script to run a DDAM analysis.

Lastly, I'd like to thank Professor Jarema Didoszak, whose expertise in both modeling and ship survivability allowed me to rapidly acquire knowledge in the complexities of naval ship shock qualifications.

THIS PAGE INTENTIONALLY LEFT BLANK

I. NAVAL SHOCK CERTIFICATION

A. CURRENT METHODOLGY

Shock certification of U.S. naval equipment began when the USN recognized that equipment failures had occurred during naval combat in WWII that were not the result of direct kinetic impacts to the vessel [1, p. 1]. Explosions from nearby ships, mines, and bombs that had missed their targets caused U.S. combat ships to lose vital equipment function, despite the fact that the vessel remained floating, stopped or less lethal in combat. In a navy where technology and investment into a smaller number of high-tech ships is preferred over a fleet of numerically superior but less advanced vessels, the loss of a single ship's ability to perform its mission capabilities can have a significant outcome on a fleet's engagement with hostile forces. The Navy's solution was to implement a shock certification program that would improve equipment survivability in the event of a non-contact, underwater explosion.

The shock certification process that has been developed is directed towards equipment survival in an UNDEX explosion. While it would be desirable to design the equipment to survive a direct or close proximity contact weapon, like a hit on a surface ship from an anti-ship missile or a contact detonation from a torpedo against a hull of a submarine, too many variables exist to effectively determine a solution directed to the survivability of the equipment. In the case of a missile strike, factors like warhead size, shrapnel distribution, thermal effects, and the resultant pressure wave generate a multitude of variables that would significantly complicate the standardization of a procedure to shock certify equipment. Adding to the complexity of the analysis are additional factors like where the missile strikes on the ship and the impact angle, the condition of the space and the surrounding spaces, and additional equipment located in the space. Furthermore, if a thorough design was engineered for a piece of equipment against such a threat index, it would be invalidated, or in this case uncertified, if the equipment location changed or the design of the weapon changed. Instead, the USN chose a more generalized approach to shock survivability by utilizing physical equipment or the DDAM modeling which creates impulses to the equipment comparable to those expected in an UNDEX event. While the

equipment may not survive a kinetic strike against the hull of a ship, it will be shock hardened to increase the probability of it surviving a warfare environment.

The current shock qualification standards are the MIL-DTL-901E and T9070-AJ-DPC-120/3010. The MIL-DTL-901E contains the physical testing used for shock qualifications and is described in Chapter II. The T9070-AJ-DPC-120/3010 covers DDAM modeling to shock qualify equipment and foundations. In the physical tests of the MIL-DTL-901E, a shock impulse is generated onto the equipment after which is evaluated to see if the equipment survived mechanically and is able to maintain its design operations and functions. Generally, the equipment is shock tested following the design of the equipment, and if a specific portion of the equipment fails testing that particular component is redesigned to ensure the overall system will repass its shock certification retesting phase. In the DDAM modeling design, a report is generated of the resultant stresses and displacements which are submitted to the appropriate technical authority specified by the acquisition documentation [2, p.7-1], and after approval, the equipment is considered shock qualified. Once the first ship of a class has been commissioned, it will undergo FSST where live fire charges will be set off in close proximity to the ship to create an underwater shock input at 2/3 of the design level of the ship [1, p. 11]. This FSST is part of the LFT&E process to ensure the survivability of the ship before the production rate of the ships is increased, as specified by the Title 10 requirement. It is important to distinguish that equipment is qualified by either the MIL-DTL-901E or the T9070-AJ-DPC-120/3010, and the FFST process is to satisfy the Title 10 survivability requirement before the production rate is increased.

B. MODELING THE FUTURE OF SHOCK QUALIFICATIONS

With advancements in modeling and the continuing increase in both the financial expense and time commitment of MIL-DTL-901E testing and the FSST process, the CNO has directed an assessment of the current methodology for shock hardening naval ships. Ongoing studies at the Naval Postgraduate School include researching the effects of an UNDEX explosion on various locations of a ship, modeling methods capable of predicting system failure, alternative physical testing available to certify equipment, and dynamic

modeling of an UNDEX explosion. The purpose of this thesis is to use the DDAM procedure, which is normally used to predict mechanical failure, to predict the functional failure of a simple system. The modeling results will be used in comparison to dynamic transient modeling, with future physical testing of the simple system to follow.

THIS PAGE INTENTIONALLY LEFT BLANK

II. CURRENT SHOCK QUALIFICATION PROCESSES

A. MIL-DTL-901E

The MIL-DTL-901E, titled *Shock Tests, H.I. (High-Impact) Shipboard Machinery, Equipment, and Systems, Requirements for*, is the governing document for naval shock requirements. It provides the categorization of different equipment and testing required for certification. The purpose of the standard is to ensure uniformity in testing between contractors over the wide range of equipment that is found on a naval vessel. The MIL-DTL-901E was revised in June 2017, the first time in 28 years, to add the Medium Weight Deck Simulating Shock Test [3, p. 38]. The MIL-DTL-901E categorizes the equipment based on factors that will affect the shock response of the equipment and the applicable testing requirements based on these classifications. An understanding of these constraints and categorization of MIL-DTL-901E is useful in determining how to apply similar assumptions in the modeling process to simplify the complexity of the shock response on a piece of equipment in the large system of a naval vessel.

1. Shock Test Selection

The first specification that determines if an item needs to be tested is its shock grade. Not all items on a naval vessel are required to be shock certified. Non-combat related components may be installed without shock certification, for example a microwave in the galley or a soap dispenser in the head or bathroom. Items that do require certification are classified with either a Grade A or Grade B shock grade. Grade A items are those "that are essential to the safety and continued combat capability of the ship," while Grade B items are those whose "operation is not essential to the safety and combat capability of the ship but which could become a hazard to personnel operating or manning Grade A equipment including personnel at battle stations, to Grade A items, or to the ship as a whole, as a result of exposure to shock" [3, p. 1]. An example of a Grade A item may be the Fire Control System for a ship's weapon system, while the folding, deck mounted chair an operator uses to man the Fire Control System may be considered Grade B. Once a contractor has verified that the equipment is Grade A or B, the acquisition documents are drafted which specify

the equipment type and class, mounting location, if the equipment will be energized or operated while testing, the type of testing machine used, the equipment mounting orientation, and others as specified in section 6.2.1 of MIL-STL-901E [3, pp. 45–46].

The equipment type is a description of the equipment as a principle unit (Type A), subsidiary component (Type B), or a subassembly (Type C). A principle unit is a large component mounted directly to the ship structure, like a gas-turbine engine. A subsidiary component is a component of a principle unit, like the motor side of a diesel generator. And a subassembly is a component associated with a principle or subsidiary component but which has no impact on the shock response of the system, like a gauge or thermometer. Generally, a system is tested as a principle unit, but a subsidiary component may be tested if it failed as part of a principle unit test, if the subsidiary component is being used on a different principle units to ensure that those principle units pass their test, or if the subsidiary component is being used on a principle unit that is requalified by shock extension. [3, p. 8]

The equipment class is a specification that describes the manner in which the equipment is mounted. The shock test machines are designed to create an input representative of an underwater non-contact explosion (UNDEX) to the shell, deck, or hull of a naval vessel. A Class I classification is equipment that is mounted to the ships foundation without any isolation device, like sound or vibration mounts. Class II equipment are those that use isolations devices, while Class I/II is used when some portions of the equipment use isolation devices whiles others do not. Figure 1 shows an example of both a Class I and Class I/II equipment.

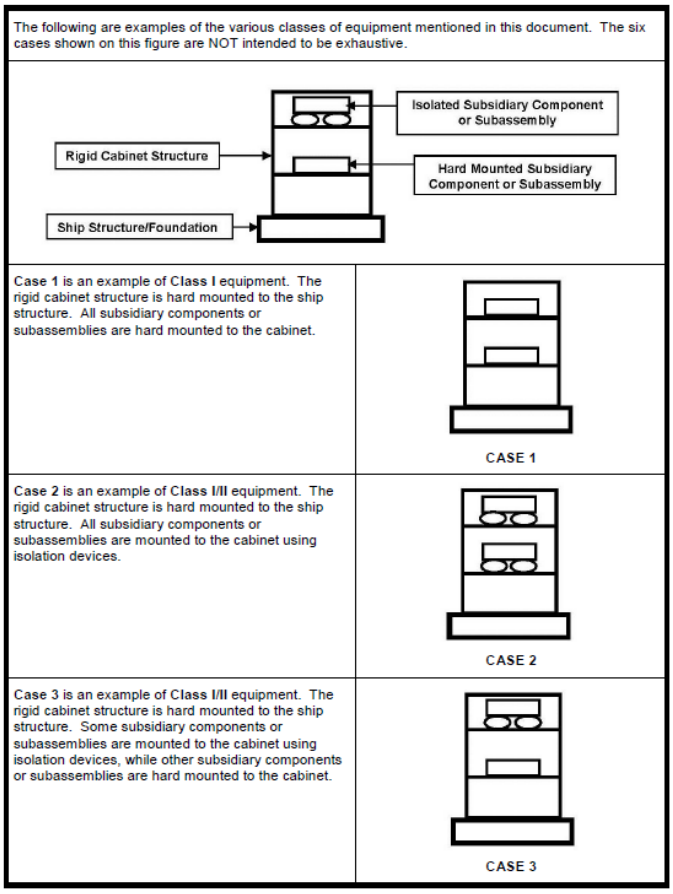

Figure 1. Class I and Class I/II. Source: [3, p. 98].

Class III equipment is similar to Class I/II in that it is a combination of isolation and non-isolation systems, but the contracting authority requires that the system be tested in both an isolated and non-isolated test.

The last major specification to be specified is the test category of the equipment. The four test categories are the lightweight, mediumweight, heavyweight, and medium weight deck simulating shock test. The test category is based on the equipment weight being tested and its class type. The lightweight test supports surface ship equipment and submarine shock mitigated deck items up to 249.48 kg (550 lb), and submarine conventional deck, hull, and frame mounted items up to 136.08 kg (300 lb) [3, p 6]. The medium weight shock test supports surface ship equipment and submarine shock mitigated deck mounted items up to 3,356.58 kg (7,400 lb) but cannot be used to test

deck mounted Class II equipment due to variances caused by the isolation properties in a Class II damped equipment. For submarine conventional deck mounted and hull mounted items, the equipment weight must be less than 2,041.17 kg (4,500 lb) with some exceptions [3, p. 7]. The heavyweight shock test is used for equipment that is larger than those in that fall into the mediumweight test and the maximum weight of the heavyweight test is dependent on which platform is used for testing. The medium weight deck simulating shock test is performed on Class II and, if applicable, Class I/II and Class III deck mounted equipment if it is between 453.59 kg and 1,814.37 kg (1,000 and 4,000 lb) [3, p. 7].

This brief overview of the MIL-DTL-901E provides a condensed summary of the method for categorizing any naval ship equipment that must be certified for a shock environment. As expected, there are numerous exceptions and clarifications for unique or infrequent testing that is listed in the MIL-DTL-901E but not mentioned in this summation. By categorizing the equipment based on location, survivability importance, isolation/dampening mounts, and the equipment weight, the MIL-DTL-901E acts as the overall guidance to certifying naval equipment against a shock event through physical testing.

2. Shock Test Machines

The lightweight shock test machine uses a 181.47 kg (400 lb) pound hammer pendulum to strike an anvil plate upon which the equipment being tested is mounted to [3, p. 62]. The hammer is dropped from heights of 0.3048, 0.9144, and 1.5239 meters (1, 3, 5 feet) depending on the ship type, class, and mounting orientation [3, p. 16]. A schematic of the lightweight shock machine is shown in Figure 2.

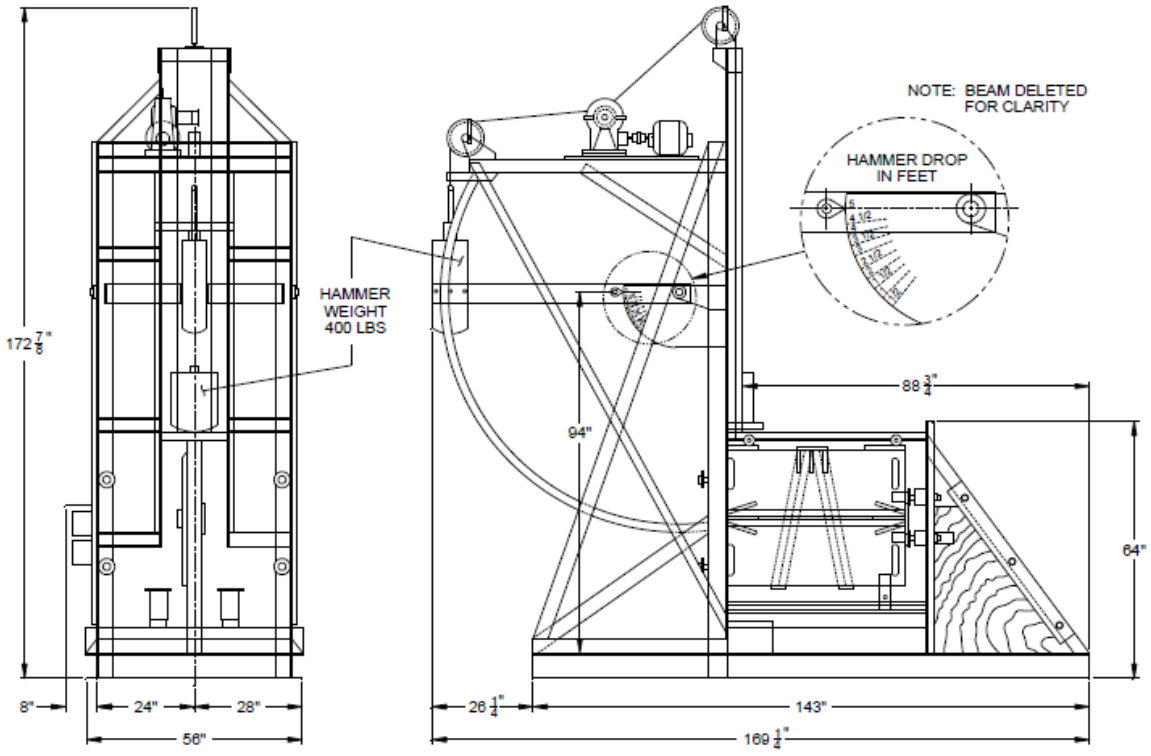

Figure 2. Lightweight Shock Machine (LWSM). Source: [3, p. 62].

Only one test is conducted at a given height and orientation. The equipment is tested in the vertical, athwartship, and fore-aft directions depending on the classification of the equipment. Once the equipment is mounted to the anvil plate, three independent hammer pendulums allow the three directional blows to be applied without having to remove and rotate the equipment being tested. An example of a LWSM test table is shown in Table 1.

Table 1. LWSM Test Schedule 1. Adapted from [3, p. 16].

Hammer Height	Test Orientation		
	Vertical	Athwartship	Fore-Aft
0.3048 meter			
0.9144 meter	X	X	X
1.5239 meter	X	X	X
Key: X denotes 1 blow			

The medium weight shock test also utilizes a pendulum hammer. Unlike the LWSM, the MWSM has a singular 1,360.78 kg (3000 lb) hammer to test equipment up to 2041.17 kg (4,500 lb) [3, p. 63]. Another importance difference is that the MWSM does not have a universal anvil plate to directly mount the test equipment. An intermediate test foundation must be installed between the test equipment and anvil plate. Because multiple orientations are required to be tested, the test equipment and foundations must be removed and reinstalled with a different foundation to test different orientations. A schematic of the mediumweight shock machine is shown in Figure 3.

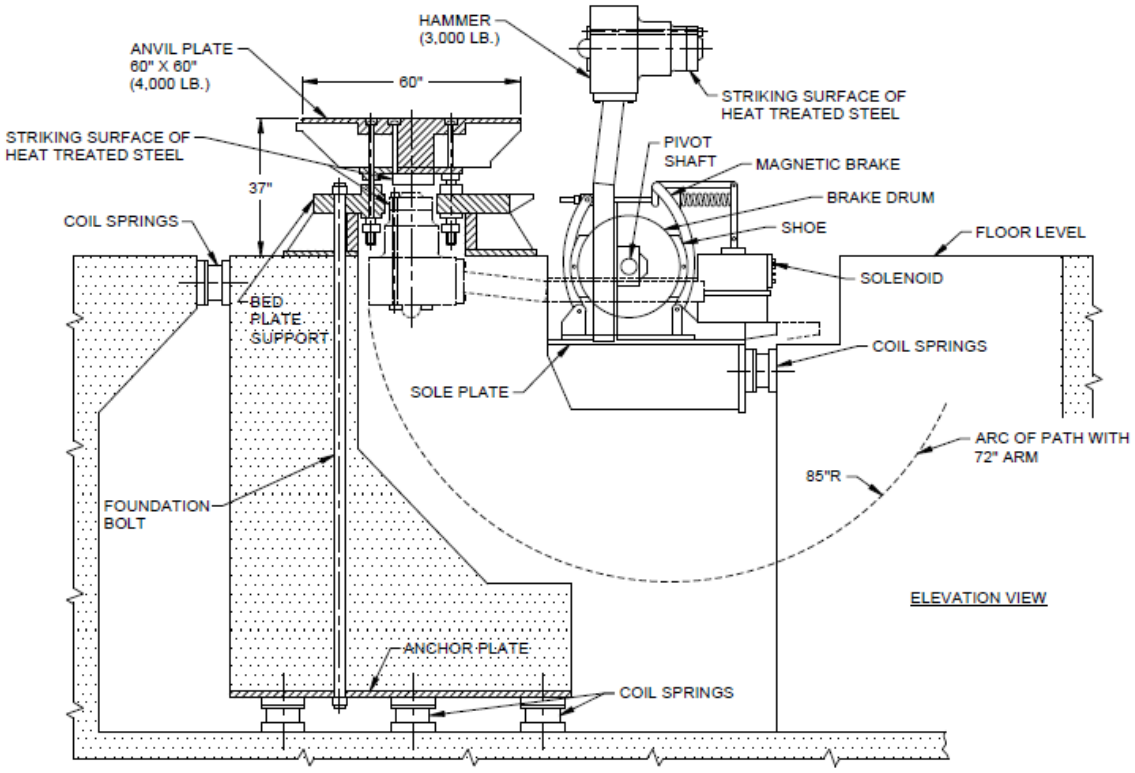

Figure 3. Mediumweight Shock Machine (MWSM). Source: [3, p. 63].

The foundations are also relatively heavy, sometimes weighting over a 450 kg themselves. Table 2 shows the required hammer drop heights based on the total weight of the test equipment and foundation. Although the equipment weight is limited to 2,041.17

kg, the table includes a total weight of 3,356.01 kg to facilitate the installation of a foundation to test the equipment [3, p. 19].

Table 2. Test Schedule for MSWM. Adapted from [3, p. 19].

Group Number	I	II	II
Number of Blows	1/	1/	1/
Anvil table travel, cm	7.62	7.62	3.81
Total weight on anvil table (kg)2/	Height of Hammer Drop (meters) 3/		
Under 453.52	0.229	0.533	0.533
453.51 - 907.03	0.305	0.610	0.610
907.03 - 1,360.54	0.381	0.686	0.686
1,360.54 - 1,587.30	0.457	0.762	0.762
1,587.30 - 1,814.06	0.533	0.838	0.838
1,814.06 - 1,904.76	0.610	0.914	0.914
1,904.76 - 1,995.46	0.610	0.991	0.991
1,995.46 - 2,086.17	0.610	1.067	1.067
2,086.17 - 2,176.87	0.686	1.143	1.143
2,176.87 - 2,267.57	0.686	1.219	1.219
2,267.57 - 2,358.28	0.762	1.372	1.372
2,358.28 - 2,448.98	0.762	1.524	1.524
2,448.98 - 2,539.68	0.762	1.676	1.676
2,539.68 - 2,811.79	0.838	1.676	1.676
2,811.79 - 3,083.90 and submarine frame mounted items 4/	0.914	1.676	1.676
3,083.90 - 3,356.01	0.991	1.676	1.676

NOTES:

1/ See tables VI through XII for number of blows per group.

2/ Total weight on anvil table is the sum of equipment weight plus weight of all mounting fixtures. Weight limits are as defined in 3.1.2.b.

3/ The height of hammer drop shall be measured by means of the existing markings on the scale of the machine, no corrections being made for the added anvil table travel for the blows of Groups I and II

4/ For submarine frame mounted items, refer to 3.1.2.b for additional details regarding weight limits on the anvil table.

The heavyweight shock test utilizes a floating platform, essentially a barge, placed in a body of water. Explosive charges are used to create a shock input to the test equipment. Different charges and floating platforms are chosen based of the size of the equipment being tested. The FSP permits the testing of large equipment, like a gas turbine or weapon system. Table 3 shows the orientation and charge variations of different FSPs.

Table 3. Test Schedule for Heavyweight Shock Test.
Adapted from [3, p. 26].

Test Conditions	Standard and Extended FSP	Intermediate FSP	Large FSP [1/]	Large FSP [1/]
Depth of explosive charge below water surface (for all shots)	7.315 meters	8.229 meters	10.972 meters	11.887 meters
Explosive charge weight of HBX-1	27.21 kg	40.82 kg	113.38 kg	145.12 kg
Direction [2/] and standoff [3/]				
Shot 1 [4/] - Fore-aft	12.19 meters	13.41 meters	21.94 meters	26.21 meters
Shot 2 -Athwartship	9.14 meters	10.36 meters	16.46 meters	19.81 meters
Shot 3 -Athwartship	7.62 meters	8.53 meters	13.72 meters	16.46 meters
Shot 4 -Athwartship	6.10 meters	6.71 meters	10.97 meters	13.11 meters
Shot 4a[5/] -Athwartship	6.10 meters	6.71 meters	10.97 meters	13.11 meters
Shot 4b[5/] -Fore-aft	[6/]			

NOTES:

1/ LFSP testing shall be performed using the 145.12 kg charge geometry column. If 145.12 kg charges are unavailable, the 113.38 kg charge geometry column shall be used. The test report shall indicate charge size, standoff distances used, and charge depth (see 6.2.3).

2/ For the fore-aft direction shots, the explosive charge shall be located relative to the FSP so as to represent an underwater explosion occurring off the bow or stern of the ship in which the equipment is to be installed. Athwartship shots shall be oriented to represent explosions abeam of the ship.

3/ Refers to the horizontal distance between the explosive charge centerline and the near ship side of the FSP.

4/ Where shot 1 is conducted, it may be the last shot performed.

5/ Where shot 4a or shot 4b is conducted, it is acceptable to omit shot 1 (see 3.1.8.3.1.b).

6/ See shot 4b on Figure 32 for standard FSP (see 3.1.8.3.1.b).

The deck of the FSP is stiffened using cross members to replicate the deck of the ship the equipment is being installed in. For environmental reasons, the testing is usually conducted

in a quarry or pond. As expected, the heavyweight shock test is the most time consuming and expensive type of testing in shock qualifications.

The last test described in the MIL-DTL-901E is the Deck Simulator Shock Machine. As previously discussed, the primary revision in MIL-DTL-901E was the addition of the DSSM in the Medium Weight Deck Simulating Shock Test. Prior to this incorporation, Class II deck equipment, i.e., deck equipment with isolators, could only be tested in a heavyweight test due to the unknown dampening effects on isolated equipment at various locations on a ship. This meant that commonly isolated deck equipment, like electronic control cabinets and controllers, had to be tested in an expensive heavyweight test despite being within the weight tolerance of a mediumweight test. In order to reduce costs, a Deck Simulator Fixture (DSF) was developed to test multiple components simultaneously in a heavyweight test between 12 to 25 Hz [4] as shown in Figure 4.

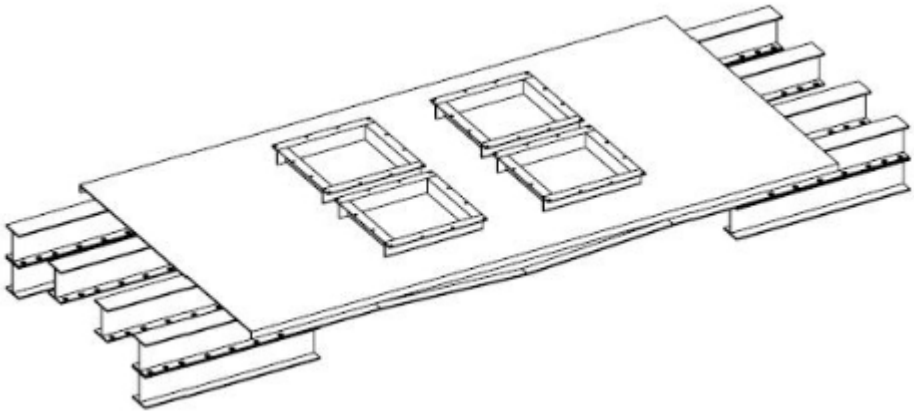

Figure 4. Navy Standard DSF. Source: [4].

While the DSF does permit the testing of multiple components, if the equipment failed it would need to be redesigned and retested in another heavyweight test. To reduce costs and allow timelier testing, the DSSM was designed. It uses a gravity drop tray and springs to test Class II, in if applicable Class II/III and Class III, equipment for deck equipment that deck locations that are expected to see less than 37 Hz [3, p. 28]. A schematic of the DSSM is shown in Figure 5.

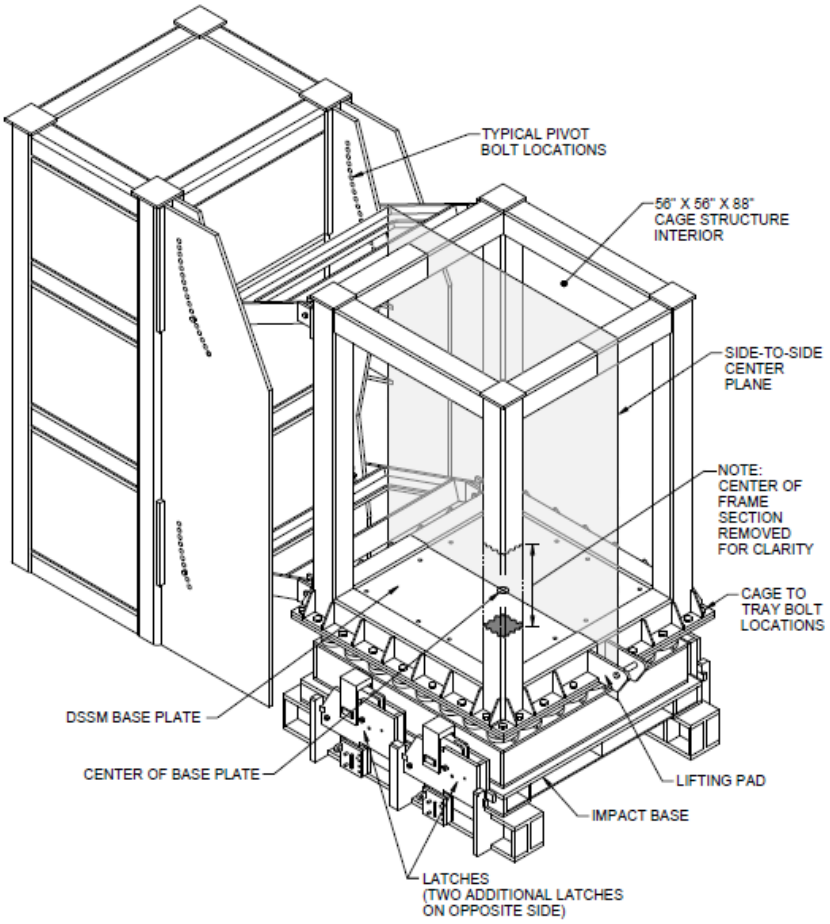

Figure 5. Deck Simulating Shock Machine (DSSM). Source: [1, p. 116].

In order to represent the appropriate shock input for the mass of the test equipment, a table is used to determine how many springs must be installed on the base plate as shown in Figure 6.

Figure 24: DSSM Tray Configuration							
Number of Springs for Tray Configuration 1							
		Class II isolated payload weight (kg; see 6.6.14.b)					
		0.00	226.76	453.51	680.27	907.03	1,088.44
Fixture weight + additional weight (kg; see 6.6.14.c and 6.6.14.d)	0	8	8	8	6 [1/]	6 [1/]	6 [1/]
	226.76	8	8	8	8 [1/]	7 [1/]	7 [1/]
	453.51	10	10	10	8	8 [1/]	7 [1/]
	680.27	10	10	10	10	8 [1/]	8 [1/]
	907.03	10	10	10	10	10 [1/]	8 [1/]
	1,133.79	10	10	10	10	10 [1/]	10 [1/]
	1,360.54	10	10	10	10	10	10 [1/]
	1,587.30	10	10	10	10	10	10 [1/]
	1,814.06	10	10	10	10	10	10 [1/]
	2,494.33	10	10	10	10	12	12

Figure 6. DSSM Spring Count for Configuration 1. Adapted from [3, p. 117].

B. DYNAMIC DESIGN ANALYSIS METHOD

DDAM is a numerical approach to yield forces, strains, and displacements on a structure or equipment. A modal analysis is performed on the structure, reducing the system to a mass-elastic system [2, p. 3–1]. The results from the modal analysis are used to generate an effective modal weight. Using coefficients determined from empirical data gathered from experimental testing, the accelerations and velocities of the system are calculated and applied to the structure, resulting in the shock input response to the system. For the purpose of this research, NRL 1396 coefficients were used. A detailed overview of the DDAM application is described in Section III.

T907-AJ-DPC-120/3010, *Shock Design Criteria for Surface Ships*, is the governing document for using the DDAM method for shock qualification. This document was revised in September, 2017 and its superseded version was NAVSEA 0908-LP-000-3010 Rev 1. The T907-AJ-DPC-120/3010 is based off the research of R.O. Belshiem and G. O'Hara in the early 1960s [2, p. 1–1]. While the DDAM process allows for equipment certification, it is primarily used for structure or foundation analysis. The first reason for this is due to

the fact that the foundations that mount the equipment to the ship are usually designed late in the ships design and construction, as the ship builder and equipment engineers will go through multiple design revisions. As such, the foundations are usually added after the ship and equipment designs have been finalized and accepted. The second is that, as previously mentioned, the DDAM analysis reduces the system to a mass-elastic system. The Navy's preference is that all physically testable equipment be tested in accordance with the MIL-DTL-901E. As a result, NAVSEA approval is required to certify operational equipment with DDAM. This preference for physical testing over modeling is shown in Figure 7 where, as long as the equipment is able to be tested on one of the physical machines previously mentioned, only NAVSEA concurrence will allow shock qualification for Grade A equipment with DDAM.

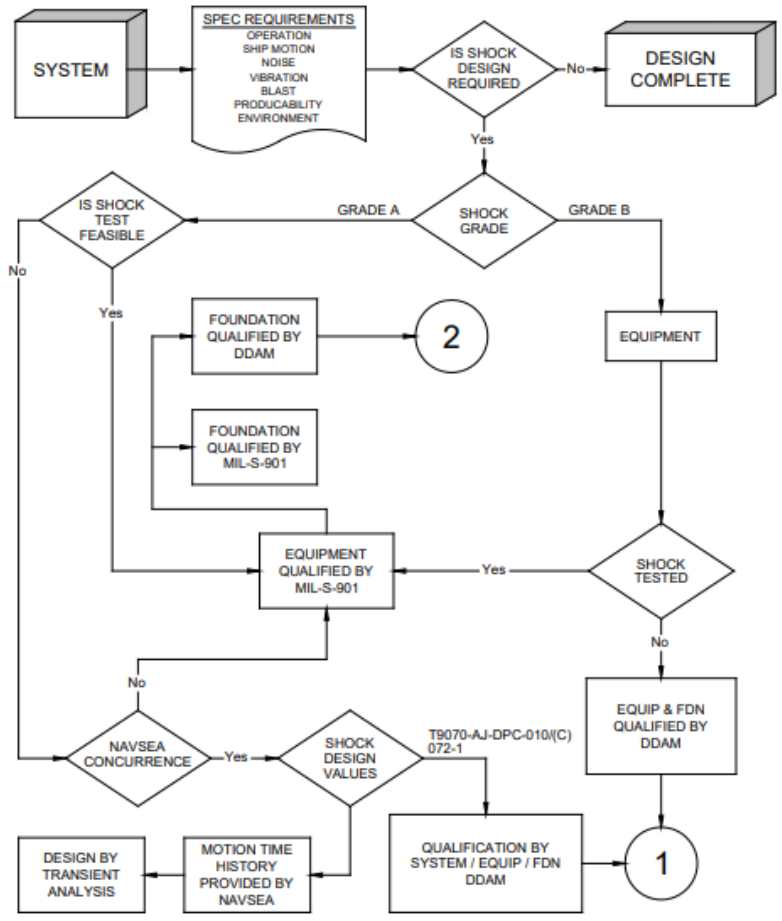

Figure 7. Selection Flow Chart for DDAM. Source: [2, p. 3–3].

C. FULL SHIP SHOCK TRIALS

The requirement for LFT&E comes from a Title 10 for program acquisitions and is a different qualification requirement than those specifying the shock hardening certifications of the MIL-DTL-901E. Under the "major systems and munitions programs: survivability testing and lethality testing required before full-scale production," Title 10 requires that the Secretary of Defense shall "provide a covered system that may not proceed beyond low-rate initial production until realistic survivability testing of the system is completed in accordance with this section and the report required by subsection (d) with respect to that testing is submitted in accordance with that subsection" [5, p. 1354]. To meet this requirement, a LFT&E phase is completed on each new class of ship. This

LFT&E includes a FSST where an operating vessel is subjected to large UNDEX events to ensure the system remains functional. This testing requires an extensive amount of resources to complete. For example, the recently built CVN-78 Gerald Ford has had its FSST schedule shuffled multiple times as the scope of the cost and removal from operation service has place an increased strain on the existing carrier fleet demand. CVN-78 was commissioned on July 22, 2017, completed its PSA in the summer of 2018, and with the addition of its shock trials and following crew certification, will not make its first deployment until 2022 [6]. This testing will cost millions of dollars, and should significant survivability vulnerabilities be found, it could significantly delay the deployment of both CVN-79 and the following CVN ships being built. In the mid 1990s, NAVSEA performed shock trials on the MHC Osprey mine hunter class. For comparison, this MHC vessel is approximately 1000 times smaller in displacement then the CVN-78. As quoted from Justin Hodge, they "had two years of post-trial design work" [7, p. 3] that was created following the testing. Although all the equipment had been shock certified with the two standards discussed previously, the survivability of the ship still required extensive redesign. While the FSST trials do identify issues prior to mass production, it also illustrates that the current shock qualification standards do not guarantee that the system will remain operational in the warfare environment.

III. DDAM

A. PERMITTANCE OF DDAM

The normal method for shock certification is through the MIL-DTL-901E process. However, there are certain situations in which shock qualification using DDAM is permissible. The two specific conditions are if a Grade A item cannot be reasonably shock tested with the MIL-DTL-901E. However, the use of DDAM must be approved by NAVSEA. The second is a Grade B item that is not required to be shock tested. The selection process is shown in Figure 7. The number of items that falls into this exception policy is limited, and majority of the items are qualified by the MIL-DTL-901E.

B. APPLICATION OF DDAM

Once the DDAM has been determined an acceptable means of qualification, coefficients are determined based on the ship type, the mounting location, and if an elastic or elastic-plastic design is required. A modal analysis is performed on the structure, and the modal participation factors P and modal weights of the system W_a^X are calculated using Equations 1 , from [8, p. 8] and Equation 2, from [9, p. 3], where M is the mass matrix, X is the modal X-directional Eigenvectors, and g is the gravitational constant with units of in/sec^2.

$$P = \sum_i \left(M_i X_{ia} \right) \tag{1}$$

$$W_a^x = \frac{g\left(\sum_i M_i X_{ia} \right)^2}{\sum_i M_i \left[X_{ia}^2 + Y_{ia}^2 + Z_{ia}^2 \right]} \tag{2}$$

The participation term is a measure of the system mass in a particular mode shape, while the modal weight of the system is the summation of the modal mass converted into units of weight. In order to simply the process, a mode reduction can be used to use modes whose summation achieves 80% of the total system mass [2, p. 3–18].

Once the modal weights are calculated, the modal accelerations and velocities are calculated by using ship type and mounting location. An example of the coefficient application to find the acceleration and velocity of surface ship hull equipment in [9, p. 4] as

$$A_o = 10.4\left[\frac{480 + W_a}{20 + W_a}\right] \tag{3}$$

$$V_o = 20\left[\frac{480 + W_a}{100 + W_a}\right] \tag{4}$$

Equation 3 results in acceleration in g while the units of velocity are in/sec. Next the directional impulse and elastic/elastic-plastic conditions are taken into place. The three impulse directions are vertical, athwartship, and fore and aft. The vertical shock impulse always has the greatest impact on the ship and has the largest weighting factor. The elastic/ elastic-plastic condition is dependent on the system type and if deformation is allowed [9, p. 10]. Table 4 shows the weighting conditions for a hull mounted equipment.

Table 4. Design Values for Hull Mounted Equipment

	Elastic		Elastic-Plastic	
	A_a	V_a	A_a	V_a
Vertical	1.0 A_o	1.0 V_o	1.0 A_o	0.5 V_o
Athwartship	1.0 A_o	1.0 V_o	1.0 A_o	0.5 V_o
Fore and Aft	0.4 A_o	0.4 V_o	0.4 A_o	0.2 V_o

With the adjusted modal accelerations and velocities, the lower of two values is used to determine the force and displacements of the system. The acceleration is converted from the units of G to m/sec^2 by multiplying by the gravitational constant. The velocity is converted from m/sec to m/sec^2 by multiplying by the modal frequency in rad/sec. If both the acceleration and adjusted velocity of a mode is less than 6 G then the acceleration for the mode is set to 6 G [9, p. 9]. To calculate the force and displacement of the system, the force is calculated with Equation 5 from [9, p. 11] and the displacement is calculated with

Equation 6 from [8, p. 19] where D_a is the minimum equivalent acceleration and ω is the modal natural frequency in rad/sec.

$$F_{ia} = M_i Y_{ia} P_a D_a \tag{5}$$

$$u_{ia} = \frac{Y_{ia} P_a D_a}{\omega^2} \tag{6}$$

Lastly, the modal forces at each node must be combined. To achieve this, DDAM uses the NRL Sum method, in which the absolute value of the largest value is selected from the modal force, and the RMS value of the remaining modal forces at each node is added to the maximum, as shown in Equation 7 from [8, p. 17].

$$\left|F_i\right| = \left|F_{ia\max}\right| + \sqrt{\sum_{i=1} F_{ia}^2 - F_{ia\max}^2} \tag{7}$$

The NRL sum is also applied in a similar manner to the modal displacements at each node. The resultant nodal forces and displacements are then used to calculate the stress and displacements of the system.

THIS PAGE INTENTIONALLY LEFT BLANK

IV. RESULTS

A. MODEL SETUP

In order to demonstrate a functional failure, a constrained system was desired where the failure mode was clearly identified and predictable. For this purpose, a square box constructed of A36 steel was modeled with two inner cantilever beams using SpaceClaim. SpaceClaim was the preferred geometry program due to its ability to model the system using shell elements instead of solid elements. This permitted 6 DOF's per node, 3 translational and 3 rotational. A spring was inserted between the two cantilever beams, which was modeled as a system connection and therefor had no mass. If the two cantilever beams come into contact with one each other via deflection, it would represent a functional failure. Due to the NRL Report 1396 using imperial units, the model was built with the units of inches and pounds. The outer shell of the system is 60.96x60.96x60.96 cm^3 (24x24x24 in^3) with a thickness of 0.63525 cm (0.25 in). The inner cantilever beam dimensions were 53.34 cm (21 in) and 22.86 cm (9 in) in length, 12.7 cm (6 in) wide, spaced 12.7 cm (6 in) apart, and 22.86 cm (9 in) from both the top and bottom of the outer shell of the model. Both beams were 2.381 cm (0.09375 in) thick. The spring connection was modeled using a 12.7 cm (6 in) spring, inserted between the beams with a stiffness of 150,000 Nm (1,327,611 lb.-in). This stiffness was based on the value used in a dynamic analysis model for comparison to the DDAM calculations. The weight of the system is approximately 111.13 kg (245 lb). Figure 8 shows the model.

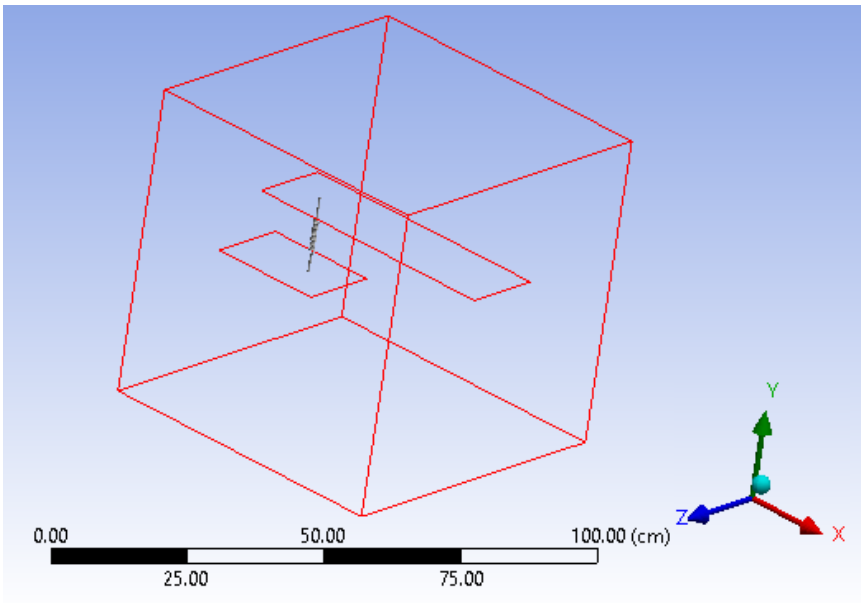

Figure 8. 60.96 cm Cube Model with Spring

The material properties were defined using the current ANSYS 18.2 engineering data for structural steel. These properties are shown in Table 5.

Table 5. Material Properties of System

Structural Steel	
Density	7.85 g/cm^3 (0.2836 lb/in^3)
Young's Modulus	200 GPa (2.90E+07 psi)
Poisson's Ration	0.3

A shell element is applied to each surface, resulting in 6 DOF's per each node. A course mesh was applied that divided each side of the outer shell into 25 elements, and divided the 22.86 cm (9 in) and 53.34 cm (21 in) cantilever beams into 2 and 4 elements, respectively. The resultant mesh yielded 156 elements with 164 nodes. Figure 9 shows the initial mesh of the model with the front Z-X plane removed.

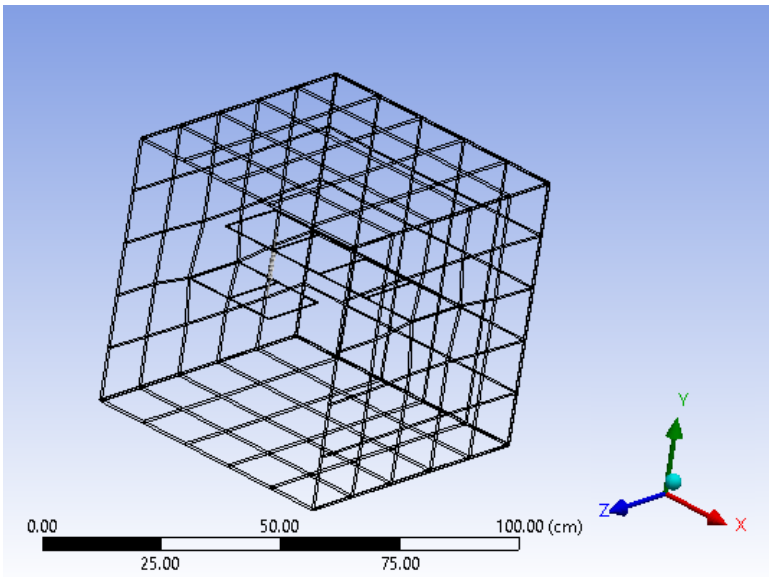

Figure 9. Mesh Application to Model

B. MODAL ANALYSIS

A modal analysis was performed on the model using ANSYS R18.2. In order to generate the mass and stiffness matrix for the model, a command prompt was made through the Commands (APDL) function, which generated the 984x984 stiffness and mass matrix for the model. A consistent mass matrix was generated as shown in Figure 10.

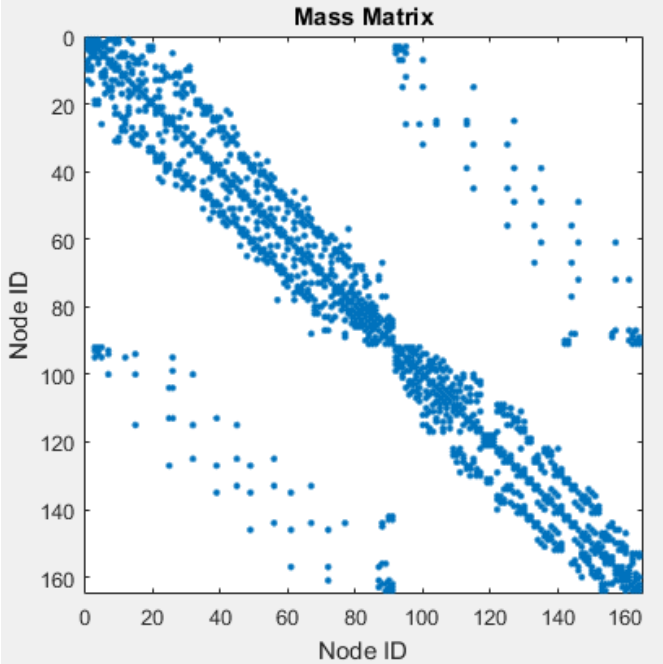

Figure 10. Consistent Mass Matrix

Constraints were then added to all for nodal corners that defined the translational displacement as 0 inches. The constraints are shown in Figure 11.

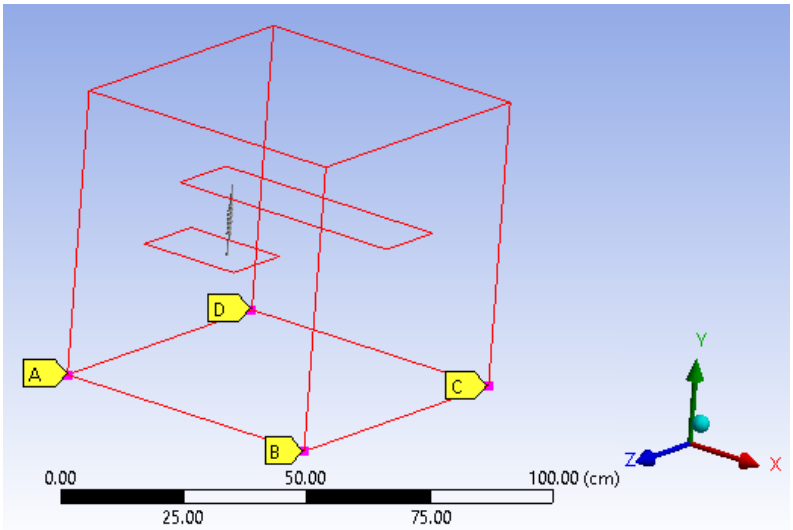

Figure 11. Constraints for Modal Analysis

One hundred modes were calculated to ensure the entire system mass was retained, resulting in a frequency range of 25.977 Hz to 3334.4 Hz with a cumulative mass of 11.352 kg sec^2/m. The modal analysis by ANSYS utilized the Block Lanczos Extraction Method with the results normalized to the mode shapes of the mass matrix. Although the frequencies and eigenvectors for simple systems could be found using the eigensolution function of MATLAB with the stiffness and mass matrix, the results found from this method began to diverge rapidly from the ANSYS modal program due to the Block Lanczos Extraction Method. As future systems where this application may be used will involve more complex systems, the numerical solution methods utilized by programs like ANSYS would be preferred due to their reduced computation time and therefor ANSYS modal results were used for the remainder of this thesis. As the system was defined to fail if the two cantilever beams contacted each other and because the vertical direction in the FSST is the most severe, only the Y direction/Vertical direction was analyzed in the DDAM calculations. Four modes were needed to achieve and 80% participation factor as shown in Table 6, listed in order of effective mass.

Table 6. Modes Required for 80% Participation Factor in Y Direction in 164 Nodal Mesh

MODE	FREQUENCY(Hz)	EFFECTIVE MASS (kg sec^2/m)	CUMULATIVE MASS (kg sec^2/m)	CUMULATIVE MASS %
40	794.02	3.2997	3.2997	29.07%
56	1067.52	2.4846	5.7843	50.95%
8	122.38	2.2396	8.0239	70.68%
55	1062.11	2.0000	10.0239	88.30%

C. DDAM RESULTS

The eigenvectors for modes 8, 40, 55, and 56 are extracted from the modal solution in the X, Y, and Z directions. The participation for the four modes are then found using Equation 1, the mass matrix, and the Y directional eigenvector. The results for the model are shown in Table 7.

Table 7. Participation Factor Results for 164 Nodal Mesh

Participation Factor	
Mode 8	0.3318
Mode 40	0.3716
Mode 55	-0.3343
Mode 56	-0.3862

The next term is the modal weight of the object which is used to determine the resultant accelerations and velocities from the DDAM design formulae. The modal weight in the Y direction is calculated as shown in Equation 8, where the X and Z eigenvector terms represent the vertical participation in the forward-aft and athwartship directions and g is the gravitational acceleration. This equation is similar to Equation 2 with the exception that Equation 8 is the modal weight in the Y direction.

$$W_a^y = \frac{g\left(\sum_i M_i Y_{ia}\right)^2}{\sum_i M_i \left[X_{ia}^2 + Y_{ia}^2 + Z_{ia}^2\right]} \tag{8}$$

The results are the modal weights for each mode. The results for the 164 nodal mesh is shown in Table 8.

Table 8. Modal Weight Results for 164 Nodal Mesh

Modal Weight (kN)	
Mode 8	0.1784
Mode 40	0.6770
Mode 55	0.3536
Mode 56	0.4341

Using the modal weight for each mode, a corresponding acceleration and velocity term are found using the reference equation for the surface ship, hull mounted, elastic condition reference equations shown in Equations 9 and 10 from [9, p. 4]. Because of the empirical nature of Equations 9 and 10, the modal weight must be in the units of kips.

$$A_o = 20\left[\frac{(37.5+W_a)(12+W_a)}{(6+W_a)^2}\right] \tag{9}$$

$$V_o = 60\left[\frac{(12+W_a)}{(6+W_a)}\right] \tag{10}$$

Because the reference equations are based on a shock wave tangential to the hull, both of the accelerations and velocities are multiplied by a constant of 1 [9, p. 5]. In order to determine which acceleration or velocity is to be used in each mode, they are converted into similar units by multiplying the acceleration by G and velocity by the modal frequency (rad/sec). The minimum of the acceleration or velocity is selected for each mode. The results of Equations 9 and 10 are shown in Table 9, while the terms in relation to acceleration are shown in Table 10.

Table 9. Modal Accelerations and Velocities in 164 Nodal

	Mode 4	Mode 40	Mode 55	Mode 56
A(G)	247.78	241.78	245.64	244.66
V(m/ sec)	3.03784	3.01041	3.02819	3.02362

Table 10. Modal Accelerations and Velocities in Terms of Acceleration in 164 Nodal Mesh

	Mode 4	Mode 40	Mode 55	Mode 56
A(m/ sec^2)	2,429	2,370	2,408	2,399
V(m/ sec^2)	2,336	15,018	20,208	20,281

From Table 10, the minimum acceleration or velocity is selected for each mode. If both of the values are less than 6 G, then the modal acceleration is set to 58.8 m/sec^2. The

nodal force is calculated using Equation 5 where P is the modal participation factor and D is the minimum modal acceleration or velocity in in/sec^2.

$$F_{ia} = M_i Y_{ia} P_a D_a \tag{11}$$

The result of Equation 11 is a matrix of 164x4, where each node has four forces. In order to find the single force at each node, and NRL sum is performed at each mode as shown in Equation 7. The results of equation produced a 164 x 1 nodal force vector which was imported into ANSYS 18.2 for a visual representation of the stress and resultant displacement based on the nodal forces as shown in Figures 12 and 13.

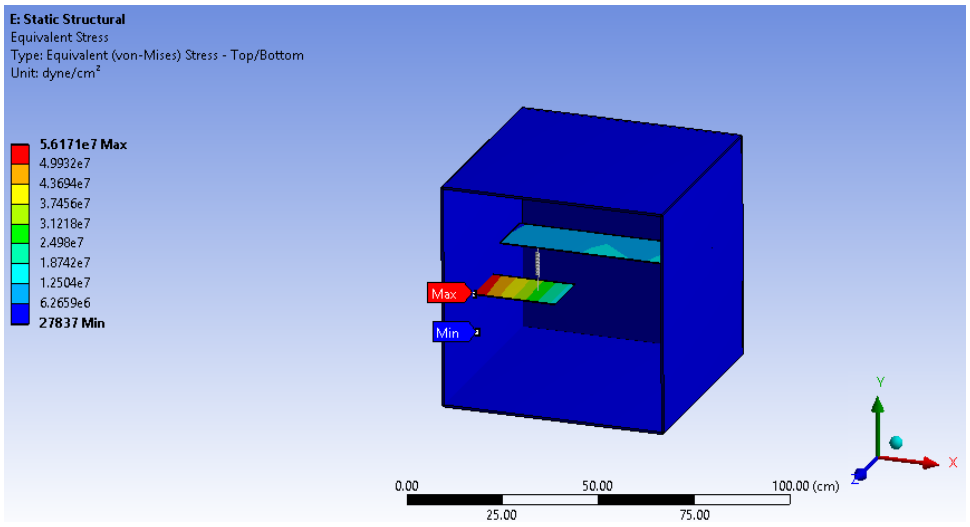

Figure 12. Stress from Nodal Forces

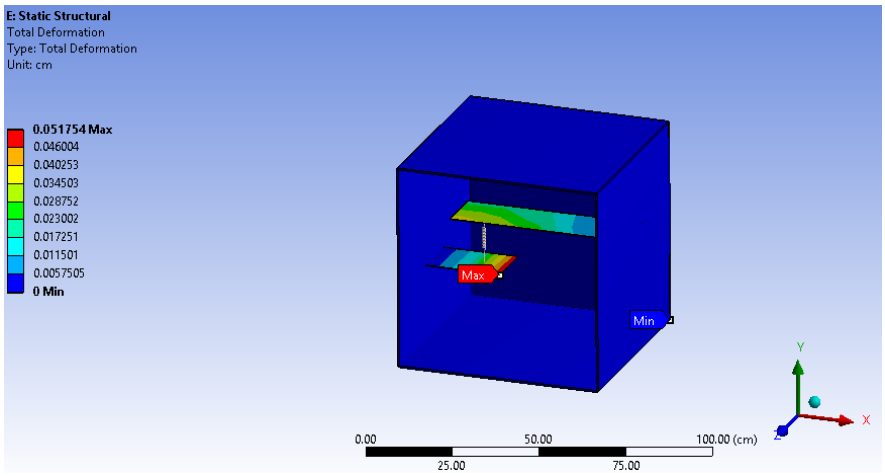

Figure 13. Displacement from Nodal Forces

D. DISPLACEMENT RESULTS

NRL Memorandum Report 1396 specifies that the displacement should not be calculated from the nodal forces [9, p. 17], as shown in Figure 13. Instead, the nodal displacements are calculated using Equation 7 as described by [8, p. 19].

$$u_{ia} = \frac{Y_{ia} P_a D_a}{\omega^2} \tag{12}$$

The result is a displacement matrix of 164 x 4. The nodal displacements are calculated using the same NRL technique of Equation 7, resulting in a nodal displacement vector of 164 x 1. The vector is imported into ANSYS 18.2 for visual representation as shown on Figure 14.

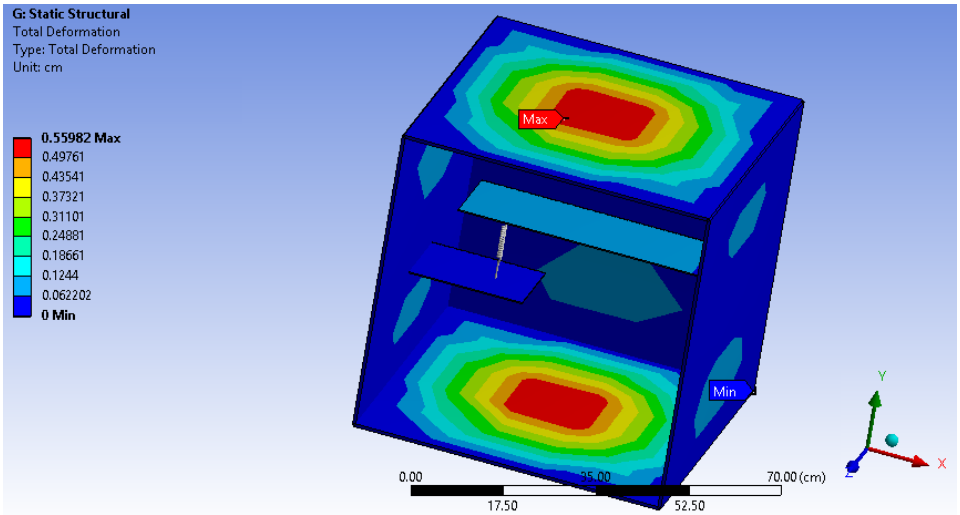

Figure 14. DDAM Displacement in 164 Nodal Mesh

The difference in displacements from Figure 13 and 14 is a result of the reapplication of the system stiffness. In the DDAM analysis, the resultant forces are calculated on a nodal basis. The stiffness of the material is factored into this resultant force vector by the material's stiffness participation in the eigenvector results. In Figure 13, the nodal forces are applied from the DDAM analysis on each node, and ANSYS calculates the resultant displacement in the structural analysis by using the system stiffness a second time. Due to the greater thickness of the outer casing, the resultant forces cause less displacement than expected. Equation 7, however, calculates the nodal displacement directly. As expected, the outer casing that is perpendicular to the applied vertical impulse applied with the DDAM coefficients have the greatest displacement. Additionally, the outer casement displacement in Figure 14 is about 10 times greater than the cantilever displacement. This is due to the upper and lower casing having larger eigenvectors in the modal solution. The results of the nodal eigenvectors from the modal analysis is shown in Figure 15.

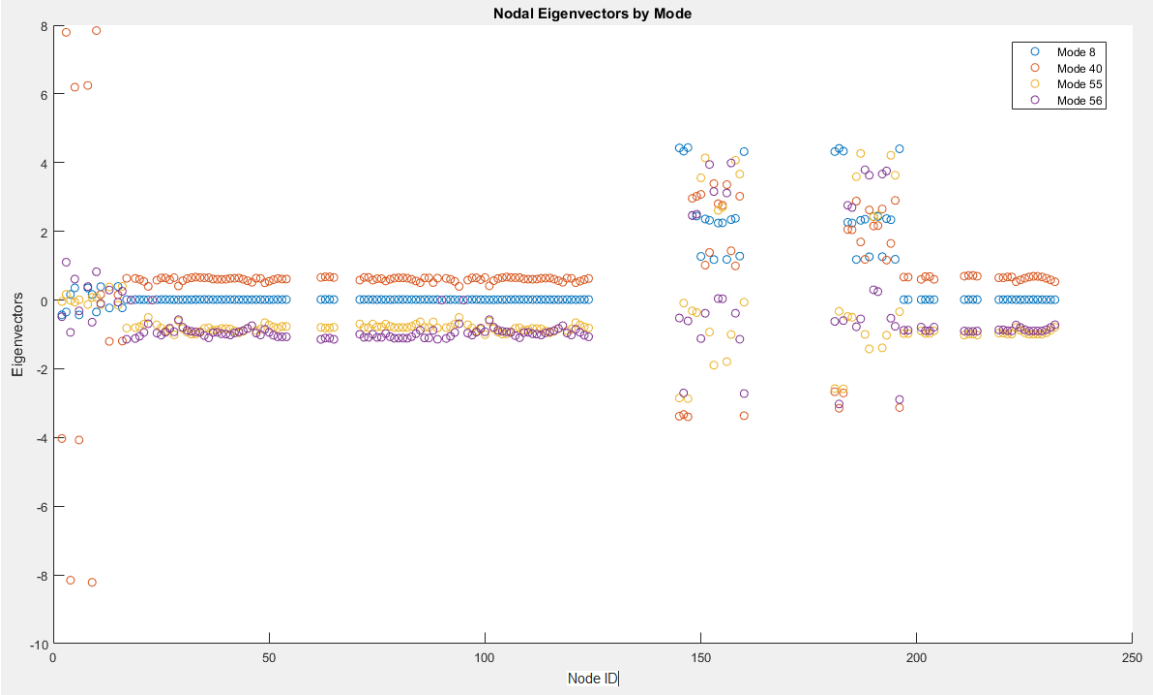

Figure 15. Nodal Eigenvector by Mode

The gaps in the plot represent where the nodes have been combined in the mesh process to ensure system interdependency. Each mode in Figure 15 has 164 data points, each representing a node in the system. The lower Node ID's represent the cantilever beams, while between the Node ID of 150 through 200 represent the center of the upper and lower system casing. Despite a few of the eigenvectors in Mode 40 on the cantilever beams having a large magnitude eigenvector, the overall eigenvector summation of the upper and lower casing nodal locations is greater. As shown in Equation 12, this causes the nodal displacements of these locations to be greater than those found in the cantilever beam.

E. SPLIT MODES

The phenomenon of a split mode is when in the modal analysis, two modal solutions are reached that contain similar in frequency and mass. Due to the NRL summation method shown in Equation 7, this may result in a potentially erroneous increase in shock loading to the system [2, p. H-7]. As seen on Table 6, mode 55 and 56 have similar frequencies and

effective masses. To identify the cause of the split mode, the system eigenvectors are plotted as shown in Figure 16.

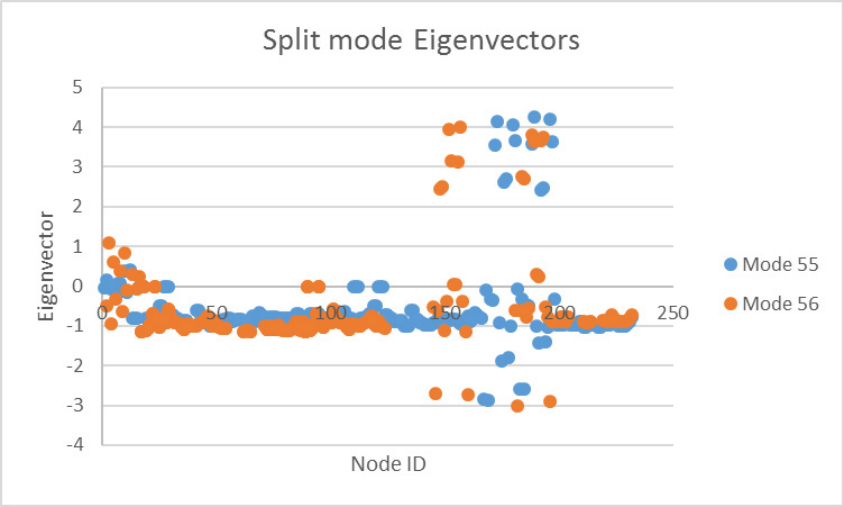

Figure 16. Plot of Mode 55 and Mode 56 in 164 Nodal Mesh

Due to the magnitude of the displacements between the Node ID locations of 150 to 200, Figure 17 was plotted to perform a trend analysis.

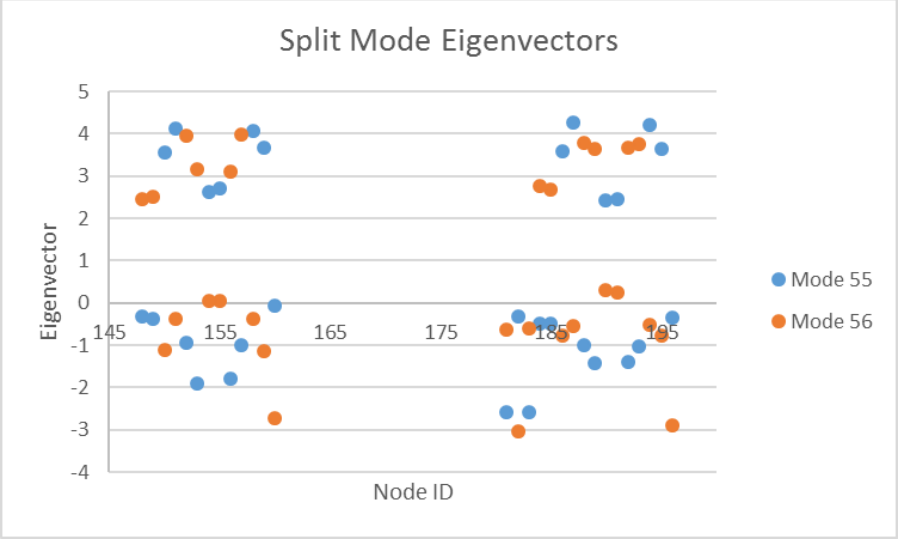

Figure 17. Plot of Mode 55 and Mode 56 in 164 Nodal Mesh between Node ID 150 to 200

Performing a trend analysis on Figure 17, a few observations can be made. The first is that the overall magnitudes are approximately the same. The second is that for any given Node ID location, when Mode 55 has a large eigenvector the Mode 56 eigenvector is low, and vice versa. The third is that, based on the nodal eigenvector displacements, the upper and lower casing have the highest participation. These patterns indicate that instead of two modes, the modal results have divided a singular mode into two subsequent modes due to the close proximity of the eigensolution. To confirm these results, ANSYS Modal was used to show these two modes, shown below in Figures 18 and 19.

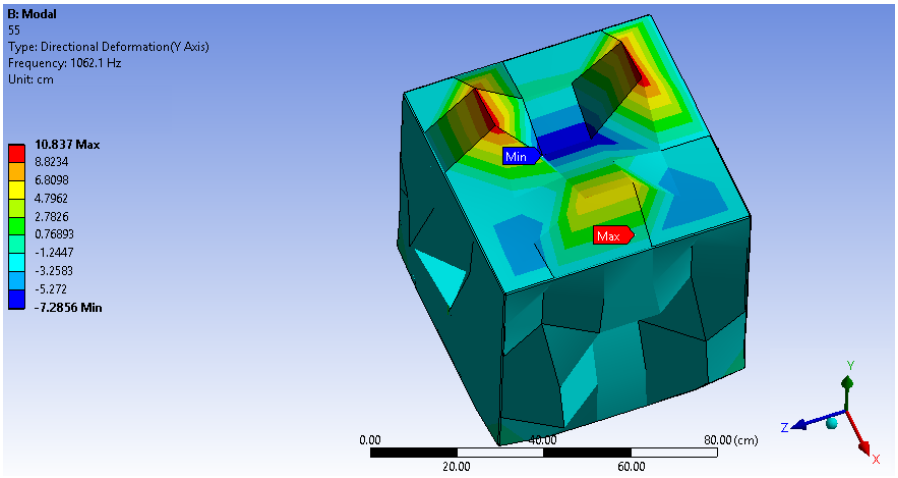

Figure 18. Mode 55 in 164 Nodal Mesh, Top View

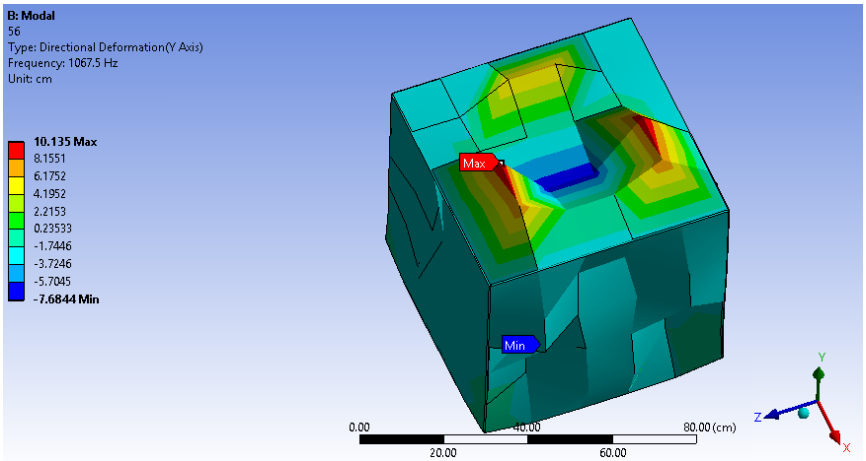

Figure 19. Mode 56 in 164 Nodal Mesh, Top View

As shown in Figures 18 and 19, the two modes represent a similar eigenvector solution rotated approximately 90 degrees about the Y axis. The bottom view of the system has a similar modal response. In order to resolve the split mode, the mesh was refined on the top and bottom of the system casing by increasing the mesh matrix on the casing from a 5x5 into a 6x6 element mesh. The results of the mesh application are shown in Figure 20.

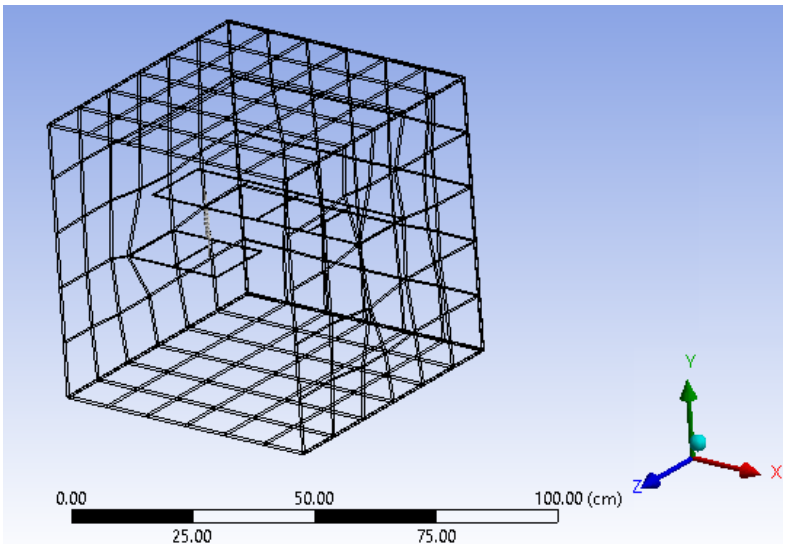

Figure 20. Mesh Refinement of Upper/Lower Casing in 204 Nodal Mesh

Performing the modal analysis of the system with the updated mesh verified that the split mode phenomenon had been removed, as shown in Table 11.

Table 11. Modes Required for 80% Participation Factor in Y Direction in 204 Nodal Mesh

MODE	FREQUENCY (Hz)	EFFECTIVE MASS (kg sec^2/m)	CUMULATIVE MASS (kg sec^2/m)	CUMULATIVE MASS %
57	1000.76	5.3482	5.3482	47.11%
39	683.04	2.3411	7.6892	67.74%
8	119.54	2.2143	9.9035	87.24%

F. FINAL MESH REFINEMENT

With the identification process of split modes and understanding of how to calculate the displacements required to determine if the system is expected to fail, the final mesh was refined in order to increase the number of nodal displacements along the cantilever beams. The degrees of freedom was increased until the difference in the modal frequencies from the previous modal analysis was less than 2%. This process is shown in Figure 21.

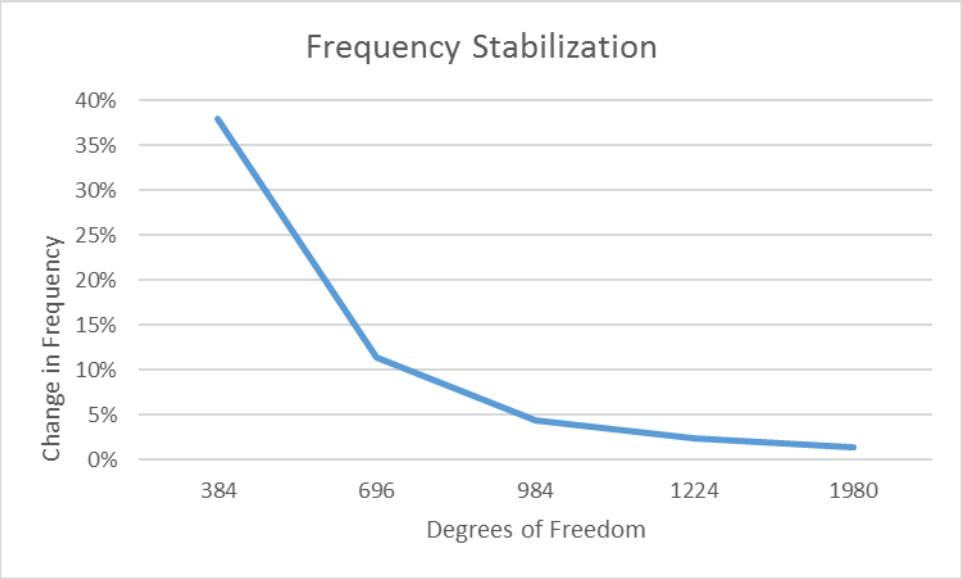

Figure 21. Frequency Stabilization with Increase DOF's

The final mesh applied to the system consisted of 321 elements and 330 nodes, which resulted in 1980 DOF's. The smaller 22.86 cm cantilever beam was modeled with 6 elements, and the longer 53.34 cm cantilever beam contained 12 elements. Each face of the casing was meshed using a 7 element by 7 element matrix. The final mesh is shown in Figure 22 with the front plane mesh removed.

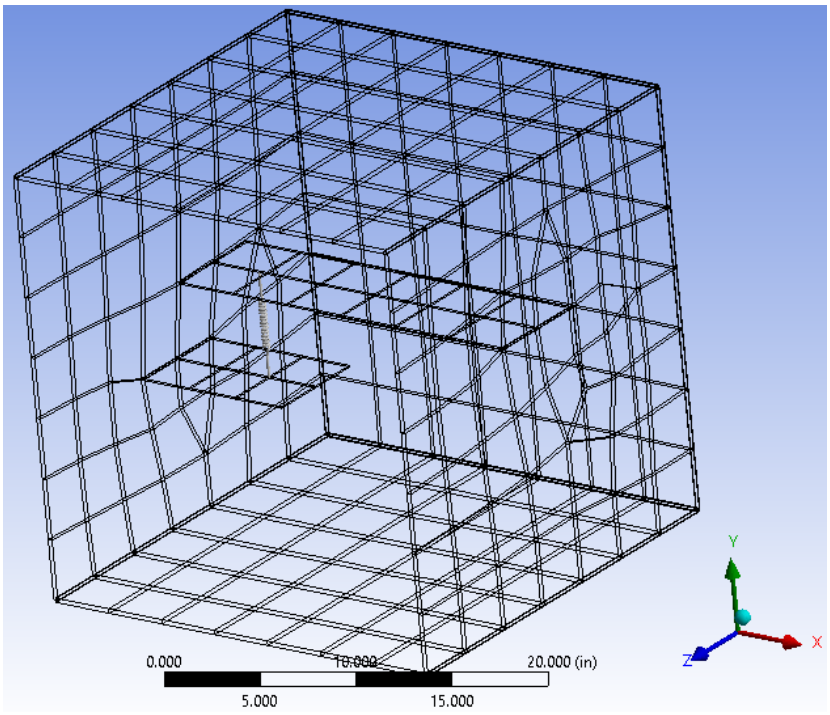

Figure 22. Final Refined Mesh in 330 Nodal Mesh

A modal analysis was performed on the system with the results shown in Table 12, with the first two mode shapes shown on Figures 23 and 24.

Table 12. Modes Required for 80% Participation Factor in Y Direction in 330 Nodal Mesh

MODE	FREQUENCY (Hz)	EFFECTIVE MASS (kg sec^2/m)	CUMULATIVE MASS (kg sec^2/m)	CUMULATIVE MASS %
70	943.6	5.3213	5.3213	46.88%
8	117.87	2.2196	7.5410	66.43%
42	599.19	1.6374	9.1784	80.85%

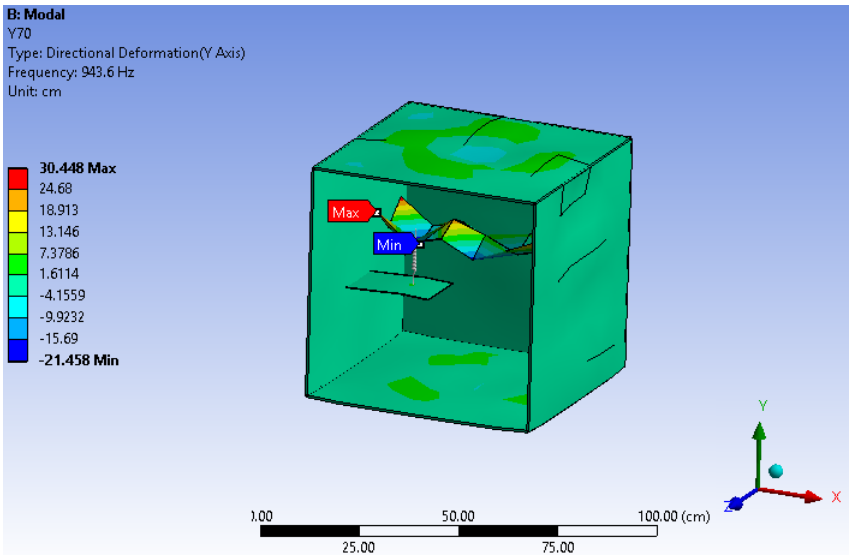

Figure 23. Mode 70 Mode Shape in 330 Nodal Mesh

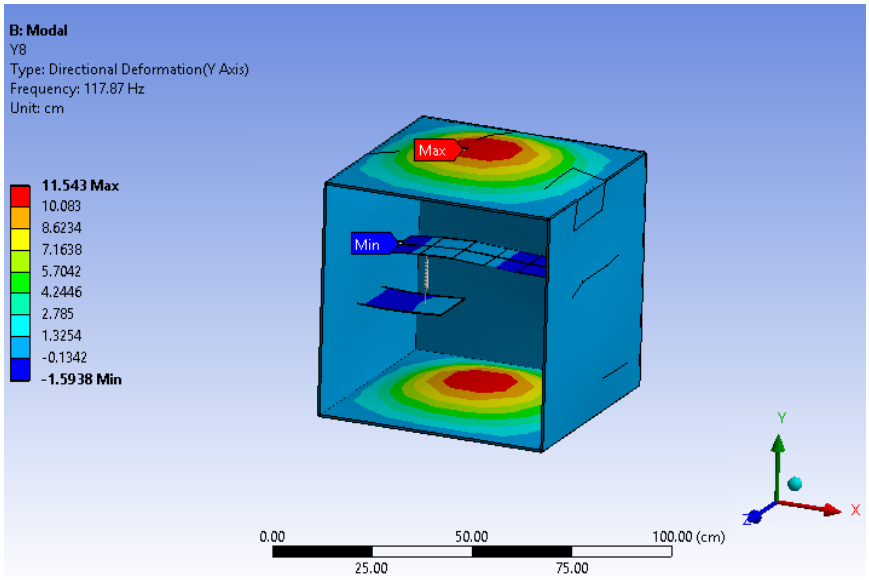

Figure 24. Mode 8 Mode Shape in 330 Nodal Mesh

Additionally, a new consistent mass matrix was generated. Using Equations 1, 8, 9 and 10, the results of Tables 13–16 were calculated in the same manner as the 164 nodal mesh model.

Table 13. Participation Factor Results for 330 Nodal Mesh

Participation Factor	
Mode 8	0.3458
Mode 42	-0.275
Mode 70	-0.4429

Table 14. Modal Weight Results for 330 Nodal Mesh

Modal Weight (kN)	
Mode 8	0.2220
Mode 42	0.1810
Mode 70	0.9239

Table 15. Modal Accelerations and Velocities in 330 Nodal Mesh

	Mode 4	Mode 42	Mode 70
A(G)	247.78	241.78	245.64
V(m/ sec)	3.0353	3.03784	2.99695

Table 16. Modal Accelerations and Velocities in Terms of Acceleration in 330 Nodal Mesh

	Mode 4	Mode 42	Mode 70
A(m/sec^2)	2,424	2,429	2,342
V(m/sec^2)	2,248	11,436	17,769

Using Equation 12 with the eigenvectors and frequencies from the modal analysis and the participation factors of Table 13 and minimum accelerations of Table 16, the nodal displacements are calculated as shown on Figure 25.

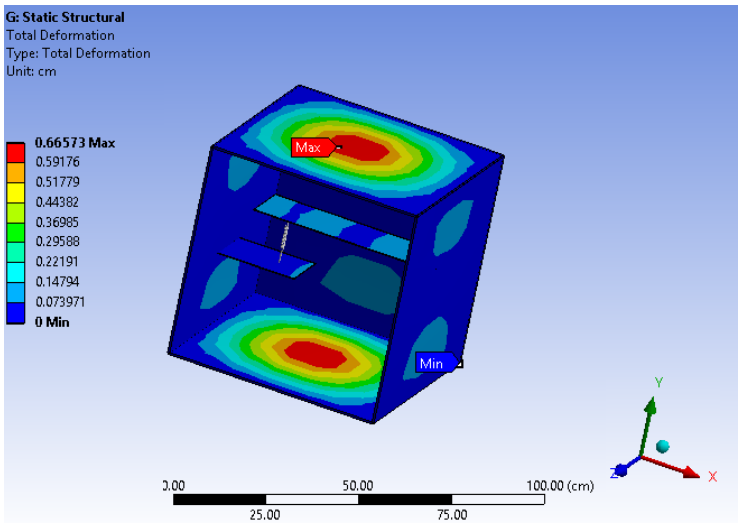

Figure 25. DDAM Displacement in 330 Nodal Mesh

As shown in the mesh of the system in Figure 22, both cantilever beams have central nodal locations along the X-axis. These individual displacements, calculated from the DDAM analysis, are shown in Figure 26.

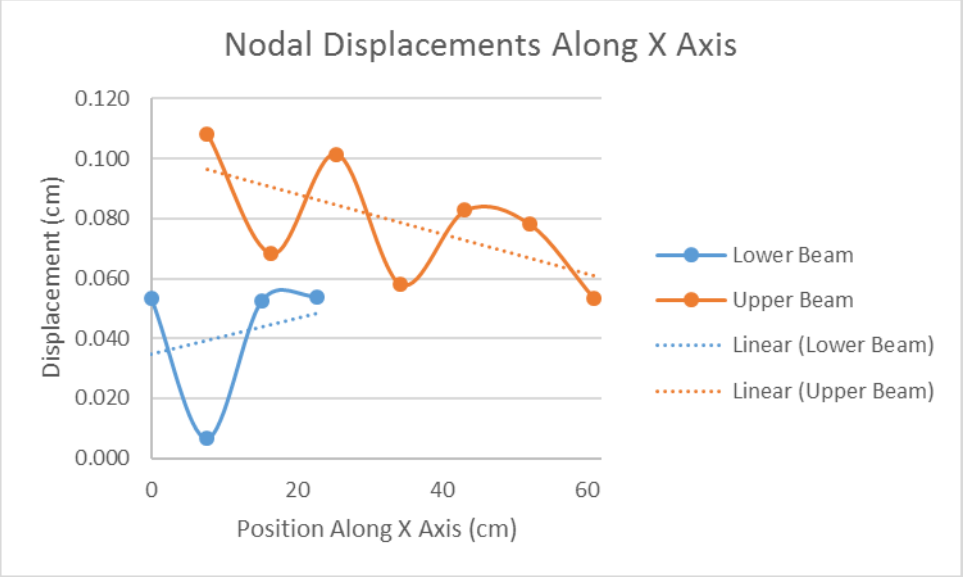

Figure 26. Cantilever Center Nodal Displacements

In reviewing Figure 26, it is observed that all of the displacements are positive. This is a result of the NRL summing method in Equation 7. Another observation is that the displacements of the cantilever beam fall above and below a linear fit line of the displacements.

Along each Z location of the cantilever beams is 3 nodes. Figure 27 shows the comparison of the three Z axis locations of the upper cantilever beam.

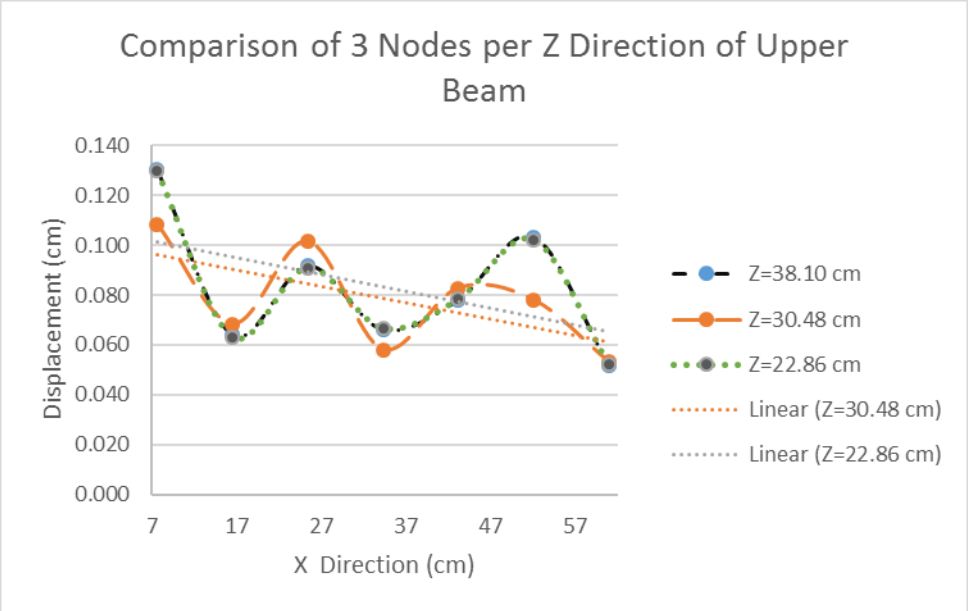

Figure 27. Nodal Displacement Comparisons of Upper Cantilever Beam

The orange line in Figure 27 is central nodal location along the upper cantilever beam shown in Figure 26. The two other lines represent +/- 7.62 cm from the central nodes, at Z=22.86 cm and Z=38.10 cm. Both of these lines have the same displacements, but are slightly different from the center nodal displacements. Additionally, a trend line between the outer nodes and center nodes shows a similar slope between the displacements.

G. COMPARISON TO DYANAMIC TRANSIENT MODELS

Previous dynamic transient modeling has been performed by NPS on a similar model. Figure 28 shows the dynamic transient modeling of the box.

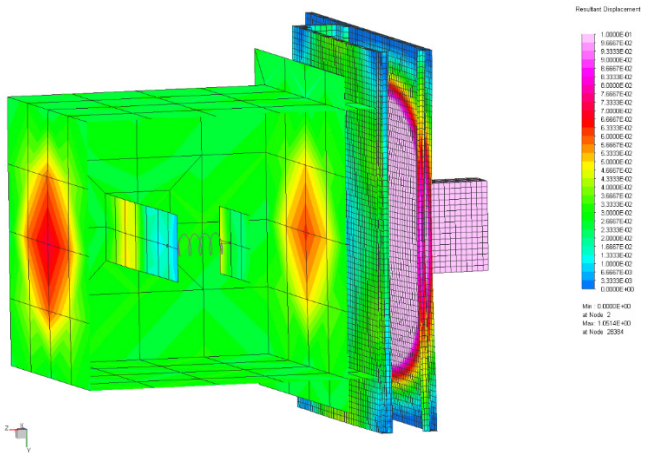

Figure 28. Dynamic Transient Modeling of System with LWSM

Because the peaks of displacement occur at different times in the dynamic transient modeling, only the maximum displacement of the system casing is shown in Figure 28. Both of the displacements of the cantilever beams and casing in the dynamic transient modeling are approximately 0.05 cm. While the displacement of the DDAM modeling matches the cantilever beam displacement, the casing displacement of the DDAM results is 0.66 cm, or 10 times greater than the dynamic transient representation of the LWSM.

Another dynamic transient modeling was performed using the FSP shock input, shown in Figure 29.

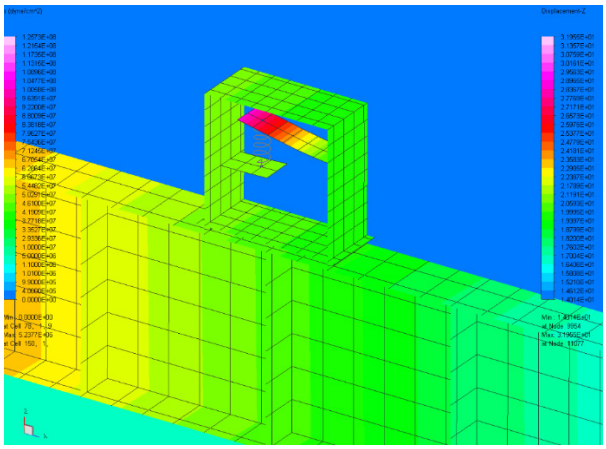

Figure 29. Dynamic Transient Modeling of System with FSP

The maximum displacement observed in the dynamic transient modeling with the FSP was about 15.24 cm, far greater than either the dynamic transient modeling of the LWSM or the DDAM analysis of the system.

V. CONCLUSION

A. IN REGARD TO DYNAMIC TRANSIENT ANALYSIS

Comparing the DDAM analysis to the dynamic transient LWSM analysis, the displacements of the cantilever beams were similar, but the casing displacement of the DDAM analysis was a factor of 10 times greater than the dynamic transient modeling. Due to more modal eigenvectors of the casing as discussed of Figure 15, the DDAM results reflect the largest displacement in the casing. In looking at the difference between the two locations, the cantilever beam is a slender beam while the casing is a plate element. The slender beam only participates primarily in one mode, while the casing participates in all three modes. The larger participation of all the modal eigenvectors of the casing result in the larger displacement results.

When equating the DDAM analysis to the dynamic transient FSP analysis, the displacements were very different. This isn't necessarily unexpected in that the impulse modeled from the FSP isn't a direct representation of the empirical data used in the DDAM analysis. Additionally, the FSP dynamic transient model did not have a tuned deck, similar to what was shown on Figure 4. The end result was that the DDAM analysis was much closer to the dynamic transient LWSM then the FSP analysis. Because the FSP is essentially a scaled-down version of the FSST UNDEX event that the DDAM analysis is supposed to represent, it is reasonable to expect the DDAM analysis and FSP analysis to yield more similar results if the FSP analysis includes a tuned deck platform.

With the displacement results from the model calculated using the DDAM process, the next step will be physical testing to gain additional information to compare to the model results. Due to the 111.13 kg design of the system, it is within the weight tolerance of the LSWM. And due to its small size, it should be feasible to mount on a FSP in conjunction with actual testing events. However, the MWSM would be the optimal testing method due to machine access and how close the model's weight is to the maximum permitted weight of the LSWM. This physical testing would allow further analysis into the displacements

the system will see and the ability to predict it with the DDAM analysis and current transient modeling techniques.

B. IN USING DDAM TO PREDICT SYSTEM FAILURE

Without physical testing, it is inconclusive if the DDAM analysis on the system, specifically the displacements, could be used to guarantee the survivability of the system. But in understanding the methodology of how the DDAM process is used, similar processes can be incorporated into future modeling. Through the years of using DDAM, issues like the split modes have been identified and incorporated into the T9070-AJ-DPC-120/3010 standard and the MIL-DTL-901E has provided a method for categorizing equipment. Modeling has advanced significantly over the years. But even with the developments in programing and computing capability, it is unrealistic to expect every design of a system to utilize a finite element model from the start of an UNDEX to a location on the ship for a shock hardening qualification. Rather, a generalized standard will need to be developed that balances the desire for more thoroughly shock hardened equipment and the complexity and costs of dynamic transient modeling, while separately verifying the results with physical testing. By using the lessons learned from the DDAM process and MIL-DTL-901E, the time is right to more heavily incorporate modeling into the shock hardening qualification and the design process.

LIST OF REFERENCES

[1] JASON, "Navy ship underwater shock prediction and testing capability study," McLean, VA, USA, Rep. JSR-07-200, 2007. [Online]. Available: https://fas.org/irp/agency/dod/jason/shock.pdf

[2] NAVSEA, *Shock Design Criteria for Surface Ships*, T9070-AJ-DPC-120/3010, Washington, DC, USA, 2017.

[3] *Shock Test, H.I. (High-Impact) Shipboard Machinery, Equipment, and Systems, Requirements for*, MIL-DTL-901E, 2017. [Online]. Available: https://www.crystalrugged.com/wp-content/uploads/2018/03/MIL-DTL-901E-DoD-detail-specification-1.pdf

[4] C. P. Milam, "Evolution of NTS' deck simulated fixtures in accordance with MIL-S-901D," National Technical Systems, August 26, 2014. [Online]. Available: https://www.nts.com/ntsblog/nts-deck-simulator-901d/

[5] Major Systems and Munitions Programs: Survivability Testing and Lethality Testing required before Full-Scale Production, U.S.C. Title 10 Part IV Chapter 139 section 2366. 2017. [Online]. Available: https://www.gpo.gov/fdsys/pkg/USCODE-2017-title10/pdf/USCODE-2017-title10-subtitleA-partIV-chap139-sec2366.pdf

[6] B. Werner, "Carrier USS Gerald R. Ford enters year-long post shakedown maintenance and upgrade period," Budget Industry, July 16, 2018. [Online]. Available: https://news.usni.org/2018/07/16/35142

[7] J. Hodge, "People: Joe Venne, program manager, underwater explosives test and trials program office," *Waves*, Issue 2, page 3, 2018 [Online]. Available: https://www.navsea.navy.mil/Portals/103/Documents/NSWC_Carderock/Waves-Issue2_2018_WEB.pdf?ver=2018-05-30-133907-133

[8] *Dynamic Design Analysis Method (DDAM) Handbook*, NEI Software,Westminster, CA, USA, 2009. [Online]. Available: http://citeseerx.ist.psu.edu/viewdoc/download;jsessionid=5AD14A11EFE35E7FC161D5E9B64EFE31?doi=10.1.1.732.1678&rep=rep1&type=pdf

[9] G. J. O'Hara and R. O. Belsheim. "Interim design values for shock design of shipboard equipment," U.S. NRL, Washington, DC, USA, NRL Memorandum Report 1396, 1963. [Online]. Available: http://everyspec.com/USN/NAVY-General/NRL_MEMO_RPT_1396_42392/

THIS PAGE INTENTIONALLY LEFT BLANK

INITIAL DISTRIBUTION LIST

1. Defense Technical Information Center
   Ft. Belvoir, Virginia

2. Dudley Knox Library
   Naval Postgraduate School
   Monterey, California